Supplementary figures and tables for "Image correlates of crowding in natural scenes"

Thomas S.A. Wallis & Peter J. Bex

April 17, 2012

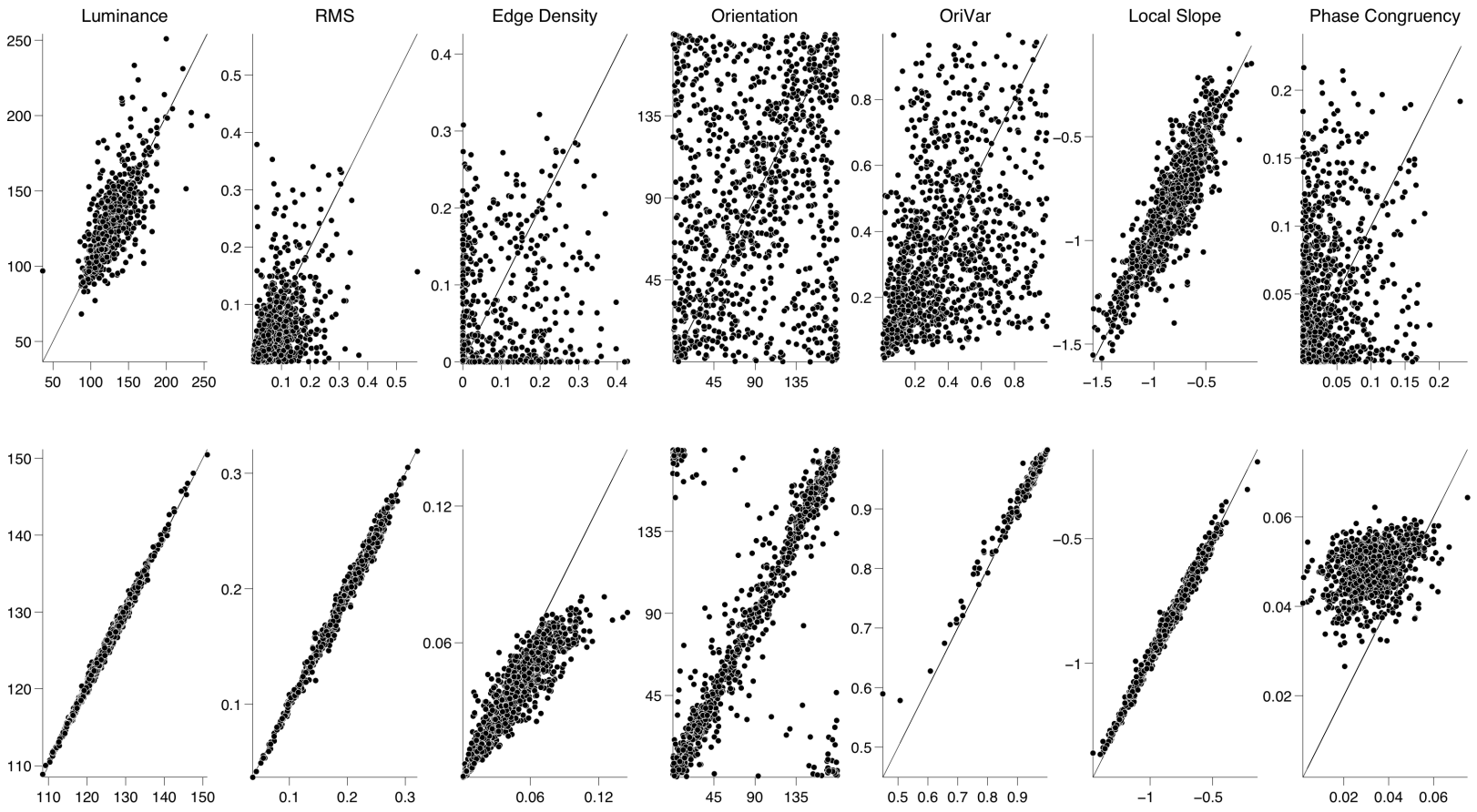

Figure S1: Dead leaves are matched on some statistics to the image patch they replace. We compared the seven image statistics of a randomly selected 750 × 750 pixel image segment from the van Hateren and van der Schaaf (1998) database with the image statistics of a dead leaves patch generated from each patch using the method described in the paper. The abscissa in all plots shows the value of the statistic for the central pixel of the natural image segment, while the ordinate shows the corresponding statistic for the "dead leaves" version of that image. Each of the 1000 points represents one such image-dead leaves pair. The first row of plots shows the value of each statistic at a fine spatial scale (Gaussian weighted average with a σ of 4 pixels). The second row shows spatially coarse statistics (σ of 128 pixels) for the same 1000 patches. Note that some of the axis ranges differ between the first and second rows to better show variation within the range of the data. The black line depicts unity (the same value for base and dead leaves images). Note that orientation is a circular variable, meaning that this plot should be thought of as lying on a sphere.

Model	Description	# Params	AIC			BIC			A_{ROC}			Posterior p		
			TW	PB	N1	TW	PB	N1	TW	PB	N1	TW	PB	N1
1	Patch Size (in decimal log of patch radius in °).	2	22687	22843	22778	22702	22859	22793	0.605	0.597	0.62	≈ 0	≈ 0	≈ 0
2	Patch Size, Eccent (2, 4 or 8 °), Patch Size and Eccent interaction	4	21945	22327	22337	21976	22358	22368	0.655	0.644	0.649	≈ 0	≈ 0	≈ 0
3	Model 2 with a quadratic term for patch size (patch^2)	5	21894	22229	22277	21933	22268	22315	0.654	0.642	0.648	≈ 0	≈ 0	≈ 0
4	Model 3 with a Patch^2 and Eccent interaction	6	21896	22226	22279	21942	22272	22325	0.654	0.641	0.648	≈ 0	≈ 0	≈ 0
5	Model 3 with categorical variable of target location (above, below, right or left of fixation), coded as 3 dummy variables	8	21669	21510	21992	21730	21571	22054	0.672	0.686	0.669	≈ 0	≈ 0	≈ 1
6	Model 3 with image segment orientation as a categorical variable	8	21898	22234	22280	21960	22295	22342	0.654	0.642	0.649	≈ 0	≈ 0	≈ 0
7	Model 5 with interaction terms between target location and eccentricity	11	21634	21428	21991	21719	21513	22076	0.674	0.691	0.67	≈ 1	≈ 1	≈ 0
8	Model 3 with target location, image orientation and interactions between target location and image orientation	20	21679	21445	21986	21833	21600	22141	0.673	0.69	0.671	≈ 0	≈ 0	≈ 0

Table S1: Candidate models for describing the influence of task parameters on performance. Eight models combining experimentally manipulated variables were tested for goodness of fit. The number of parameters for each model includes a constant term. Goodness of fit metrics provided are the Akaike Information Criterion (AIC), Bayesian Information Criterion (BIC), area under the receiver operating curve (A_{ROC}) and the BIC-approximated posterior probability of the model (Posterior p) relative to all other models, assuming that all models are equally likely *a priori* (see Wagenmakers 2007, equation 11). For TW and PB, Model 7 is strongly preferred. For N1, Model 5 is strongly preferred. Both coarse and fine exclusion rules for RMS contrast produced the same substantive conclusions.

Model	Description	# Params	AIC			BIC			A_{ROC}			Posterior p		
			TW	PB	N1	TW	PB	N1	TW	PB	N1	TW	PB	N1
1	Best task factor only model (Table 1, Model 7; Model 5 for N1)	11 (8)	21634	21428	21992	21719	21513	22054	0.674	0.691	0.669	0.5	0.5	0.5
2	Luminance added to model 1.	19 (16)	21267	21015	21785	21414	21162	21909	0.696	0.712	0.683	≈ 1	≈ 1	≈ 1
3	Contrast (as decimal log of RMS contrast) added to model 1.	19 (16)	19584	19342	20141	19731	19489	20265	0.766	0.775	0.753	≈ 1	≈ 1	≈ 1
4	Edge Density added to model 1.	19 (16)	19818	19748	20511	19964	19895	20635	0.751	0.755	0.736	≈ 1	≈ 1	≈ 1
5	Orientation at every scale (0-180 degrees) relative to screen coordinates, added to model 1.	27 (24)	21646	21438	22003	21855	21647	22189	0.676	0.692	0.671	≈ 0	≈ 0	≈ 0
6	Orientation at every scale (0-180 degrees) relative to image coordinates, added to model 1.	27 (24)	21648	21443	22007	21857	21652	22193	0.675	0.692	0.67	≈ 0	≈ 0	≈ 0
7	Orientation variance added to model 1.	19 (16)	21124	20999	21487	21271	21146	21611	0.704	0.714	0.698	≈ 1	≈ 1	≈ 1
8	Amplitude spectrum slope added to model 1.	19 (16)	20126	19922	20618	20273	20069	20742	0.742	0.753	0.733	≈ 1	≈ 1	≈ 1
9	Phase congruence added to model 1.	19 (16)	21004	20851	21474	21151	20998	21598	0.706	0.717	0.696	≈ 1	≈ 1	≈ 1

Table S2: Individual image predictors added separately to the best task parameter model. From Table S1, the best description of task parameters was model 7 for TW and PB, and model 5 for N1. Consequently, here N1 has fewer parameters than the other observers (the number of parameters for observer N1 are given in parentheses). Based on pilot analyses (not shown), here we choose to add each predictor at each of the four scales, as well as interaction terms between eccentricity and the predictor at each scale. Note that orientation is entered as two columns (sine and cosine of the orientation in degrees) and so has double the number of parameters. Goodness of fit metrics as in Table S1, with the exception that the posterior probability of each model is expressed relative to the task parameter only model (Model 1; see Wagenmakers 2007, equation 12). The coarse RMS exclusion rule produces the same substantive conclusions, but under the fine RMS exclusion rule, luminance and local slope drop out as important for TW, luminance and orientation variance drop out for PB, and luminance, local slope and phase congruence drop out for N1.

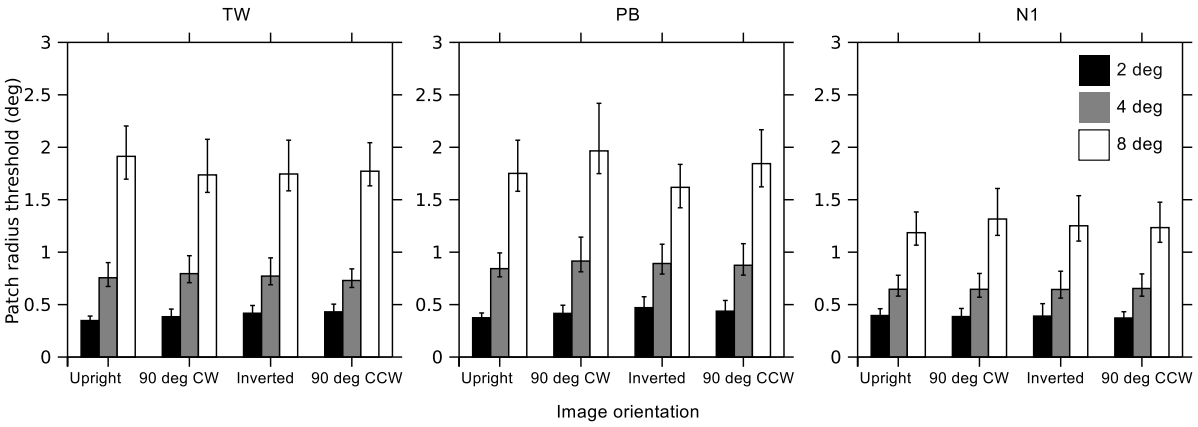

Figure S2: Threshold patch radius (degrees) for each observer as a function of eccentricity and the orientation of the underlying image segment presented on that trial. Here, performance was fitted as a function of patch size using the psignifit (version 2) toolbox (Wichmann & Hill, 2001). Error bars show 95% bootstrapped confidence intervals on the threshold. As can be seen, the underlying image orientation has no consistent influence on task performance, in keeping with the model selection results reported in Table S1, Model number 6.

Rank	Image predictor (model number)
1	RMS contrast (3)
2	Edge density (4)
3	Amplitude Slope (8)
4	Phase congruence (9)
5	Orientation variance (7)
6	Luminance (2)

Table S3: Image predictors that significantly improve model fit from the task parameter model, in order of magnitude of improvement as measured by BIC. Model number corresponding to Table S2 is shown in parentheses. All observers showed the same ranking of image predictors. Under the coarse RMS exclusion rule, the ranking of phase congruence (model 8) and orientation variance (model 7) were swapped for observer N1. Under the fine RMS exclusion rule, the model ranks changed more significantly. For all observers, edge density now ranks above RMS contrast. For TW, the model numbers of those models ranked above task parameters alone were [4, 3, 7, 9], for PB [4, 3, 9, 8] and for N1 [4, 3, 7, 1].

Model	# Params			AIC			BIC			A_{ROC}			Posterior p		
	TW	PB	N1	TW	PB	N1	TW	PB	N1	TW	PB	N1	TW	PB	N1
1	11	11	8	21634	21428	21992	21719	21513	22054	0.674	0.691	0.669	≈ 0	≈ 0	≈ 0
2	19	19	16	19584	19341	20141	19731	19489	20265	0.766	0.775	0.753	≈ 1	≈ 1	≈ 1
3	27	27	24	19377	19196	19959	19586	19405	20145	0.771	0.778	0.759	≈ 1	≈ 1	≈ 1
4	35	35	32	19365	19115	19944	19636	19386	20192	0.772	0.781	0.76	≈ 0	≈ 1	≈ 0
5	43	43	40	19293	19054	19893	19626	19386	20203	0.774	0.783	0.762	0.992	0.45	0.004
6	51	51	48	19287	19051	19900	19682	19446	20273	0.775	0.783	0.762	≈ 0	≈ 0	≈ 0
7	59	59	56	19286	19053	19878	19742	19509	20313	0.775	0.784	0.763	≈ 0	≈ 0	≈ 0

Table S4: Sequentially adding image predictors to task parameter model (here, model 1). Individually significant image predictors are added in order of importance (see Table S3) for each observer. We choose the "best" model for each observer as the one with the lowest BIC (highest posterior probability). For observers TW and N1, this is model 3, whereas for PB this is model 4. That is, the best model for TW and N1 include RMS contrast and edge density in addition to task factors, whereas for PB, amplitude spectrum slope can also be included. Under the coarse RMS exclusion rule, PB's preferred model was 5 rather than 4. That is, both local slope and phase congruence were useful for PB. Under the fine RMS exclusion rule, if predictors are entered in the original rank order (i.e. same as full dataset), then the same models are preferred as in the full dataset. If predictors are entered in their new preferred order (i.e. edge density, then RMS, etc.), the preferred model for TW is model 2 (i.e. just adding edge density), the preferred model for PB is 4 (edge & RMS & phase), and the preferred model for N1 is 3 (edge & RMS). In summary, if up to 45% of the trials are excluded based on low RMS, some divergent results in the model selection occur. Edge density becomes of primary importance relative to RMS, and preferred models diverge across observers – but for 2 of 3, both RMS and edge density are still included. Furthermore, examining plots of centre-surround fits to RMS and edge density produces similar results and the same conclusions as the full dataset.

Observer	AIC	BIC	A_{ROC}	BIC null model
TW	19378	19587	0.771	23270
PB	19197	19406	0.778	23352
N1	19959	20168	0.760	23612

Table S5: Preferred model fit for all observers. For simplicity from Table S4, we fit all observers' data with a 27 parameter model, combining task factors (including visual field location by eccentricity interactions) with $\log_{10}$(RMS contrast) and edge density. In addition, here we include the BIC for the null hypothesis (a model containing only the constant). All fitted models are preferred to the null hypothesis.

	Eccent 2				Eccent 4				Eccent 8			
Scale σ	0.0625	.25	1	4	0.0625	.25	1	4	0.0625	.25	1	4
TW	0.53	0.75	-0.15	-0.02	0.42	0.61	0.13	-0.12	0.24	0.37	0.69	-0.36
PB	0.31	0.92	-0.12	-0.09	0.27	0.56	0.41	-0.18	0.22	-0.15	1.54	-0.40
N1	0.83	0.81	-0.30	-0.06	0.63	0.65	0.00	-0.18	0.25	0.38	0.61	-0.46

Table S6: Delta logits for RMS contrast at four spatial scales (see Figure 4A for absolute values of same at 12 scales).

	Eccent 2				Eccent 4				Eccent 8			
Scale σ	0.0625	.25	1	4	0.0625	.25	1	4	0.0625	.25	1	4
TW	-0.22	0.51	-0.09	0.58	-0.19	0.34	-0.03	0.68	-0.13	0.02	0.09	0.84
PB	-0.07	0.34	-0.29	0.76	-0.14	0.36	-0.25	0.73	-0.26	0.39	-0.17	0.63
N1	-0.22	0.15	0.00	0.53	-0.22	0.26	-0.24	0.78	-0.25	0.53	-0.78	1.19

Table S7: Delta logits for edge density at four spatial scales (see Figure 4B for absolute values of same at 12 scales).